Revista EIA, ISSN 1794-1237 Número 8, p. 37-47. Diciembre 2007
Escuela de Ingeniería de Antioquia, Medellín (Colombia)

BOLTED TIMBER JOINTS WITH SELF-TAPPING SCREWS

César Echavarría*

ABSTRACT

The use of self-tapping screws with continuous threads in the joint area as a reinforcement to avoid splitting of timber members is studied. A theoretical model is developed to calculate the stress distribution around a pin-loaded hole in a timber joint, to predict brittle failure modes in bolted connections and to calculate the load in the reinforcing screws. Laboratory experiments on reinforced and non-reinforced timber joints with 15,9-mm bolts have shown good agreement with the model predictions.

KEYWORDS: timber joints; brittle failure mode; reinforcement perpendicular-to-grain; analytical model.

RESUMEN

En este artículo se estudia el uso de tornillos autoperforantes como refuerzo para evitar rupturas frágiles en uniones de madera. Se presenta un modelo teórico para calcular la distribución de esfuerzos alrededor de un perno en una unión de madera, predecir las rupturas frágiles y evaluar el esfuerzo en los tornillos autoperforantes. Los experimentos de laboratorio con uniones de madera, con pernos de 15,9 mm de diámetro, reforzadas y no reforzadas mostraron la efectividad del modelo teórico propuesto.

PALABRAS CLAVE: uniones de madera; ruptura frágil; refuerzo perpendicular a las fibras; modelo analítico.

* Ingeniero Civil, Universidad Nacional de Colombia; Master in Timber Structures and Docteur en Sciences, École Polytechnique Fédérale de Lausanne, Switzerland. Ph.D. Researcher, Département des sciences du bois et de la forêt, Université Laval, Québec. cesar.echavarria@sbf.ulaval.ca Associate Professor, Faculty of Architecture, School of Construction, Universidad Nacional de Colombia. caechavarrial@unal.edu.co

Artículo recibido 31-VIII-2007. Aprobado 11-XI-2007
Discusión abierta hasta junio de 2008

1. INTRODUCTION

It is known that the problem of mechanically fastened joints in timber is difficult to analyze because of the anisotropic and heterogeneous nature of the material. Since there are no available analytical solutions associated with loaded holes in wood, current design procedures for mechanical fasteners are based on approximate or empirical solutions and exist only for the simplest types of joints.

Due to the importance of the problem, bolted joint has been studied by using numerical and experimental [4, 7-10, 21, 22, 26, 29, 31, 32] methods in the past.

Patton-Mallory *et al*. [27] developed and evaluated a three-dimensional numerical model of a bolted wood connection loaded parallel to grain. Nonlinear parallel to grain compression of wood and degradation of shear stress stiffness were described using a trilinear stress-strain relationship. The connection model also accounted for an elastic-perfectly plastic steel pin, oversized hole, and a changing contact surface at the pin-hole interface. The numerically predicted load-displacement curves were stiffer than the experimental curves.

In Kharouf *et al*. [19], a nonlinear numerical model is developed to study the behaviour of timber connections with relatively low member thickness-to-fastener diameter ratios. A plasticity-based compressive constitutive material model is proposed to represent wood as elastoplastic orthotropic material in regions of biaxial compression. Linear elastic orthotropic material response was used otherwise with maximum stresses taken as the basis for predicting failure criteria. Nonlinear geometry due to increased sliding contact between the bolt and the hole is modelled using the Lagrange multiplier algorithm.

Jorissen [18] attempted to account for brittle fracture in timber joints using the European Yield Model by calculating stress distributions along potentially critical load paths within the wood member. The average stresses for tension perpendicular-to-grain and for shear stresses were compared with those from a fracture mechanics model to predict ultimate strength. Jorissen [18] found, however, that the tensile stresses perpendicular-to-grain were underestimated and, to allow crack initiation to be detected by the fracture theory, added an assumed peak stress perpendicular-to-grain at the bolthole location. The joint area including the stable crack propagation was modelled as a beam on elastic foundation. This assumption limits the robustness of the model.

Moses [23] and Moses and Prion [24] proposed a material model that is based on orthotropic elasticity, anisotropic plasticity for non-linear behaviour of wood in compression, and the Weibull's weakest link theory to predict brittle failure. Linear elastic behaviour was assumed for tension and shear. The weakest link theory provides a probabilistic approach to predicting the failure based on the stressed volume of wood and can be used for cases when the ultimate strength of the single bolt connection is governed by brittle failure (such as shear and tension perpendicular-to-grain). This three-dimensional model was implemented using finite element analysis for a single-bolt connection specimen.

Regrettably, experiments and numerical methods do not produce open-form solutions as a result of the high amount of possible combinations of involved parameters. In contrast, it would be practical to have equations developed using the detailed analytical basis.

The objective of this paper is to present a comprehensive analytical method capable of predicting the ultimate strength of reinforced and non-reinforced timber bolted joints. The method of complex functions [20, 25] for anisotropic materials is used to obtain the stress distributions. The solution is compared directly to results of laboratory tests.

This study examined as well the technical feasibility of reinforcing the wood at bolted joints with self-tapping screws. The purpose of local reinforcements in a joint is to improve its load-carrying capacity and stiffness and to improve its ductility.

This paper reports test results of various connection configurations with reduced end distances, with and without reinforcement.

2. STRESS DISTRIBUTION AROUND A PIN-LOADED HOLE IN AN ELASTICALLY ORTHOTROPIC PLATE

In this paper, the stress distribution around a pin-loaded hole in an elastically orthotropic plate is investigated for the main member of a double-lap mechanically fastened joint. Consider a homogeneous, orthotropic plate of width *b* with a circular hole of diameter *d* as is shown in Fig. 1. Let the *x*- and *y*-axes be the principal axes of the plate, and the direction of the pin load *F* be the same as the positive *y*-axis. The hole is at a distance *e* from the free end of the plate. The clearance between the pin and the hole is denoted as λ.

The pin-hole problem is essentially a two-body-contact problem. In order to determine contact surfaces and stresses the inverse method is used, a value for the contact angle between the bolt and the timber is assumed and the corresponding load is calculated. The process is repeated for a series of prescribed contact angles. The assumption of a value for the contact angle has the advantage of simplicity.

It is assumed that the hole is loaded without friction on a portion of its edge by an infinitely rigid pin of diameter *d*. The loading pin is represented by compressive edge loads distributed around the hemispherical contact area. The resulting force *F* equals *2pRt*, where *p* is the average bearing stress according to the classical definition, *R* is the radius of the hole and *t* is the unit thickness of the plate. The analytical model with its boundary and loading conditions is shown in Fig. 2.

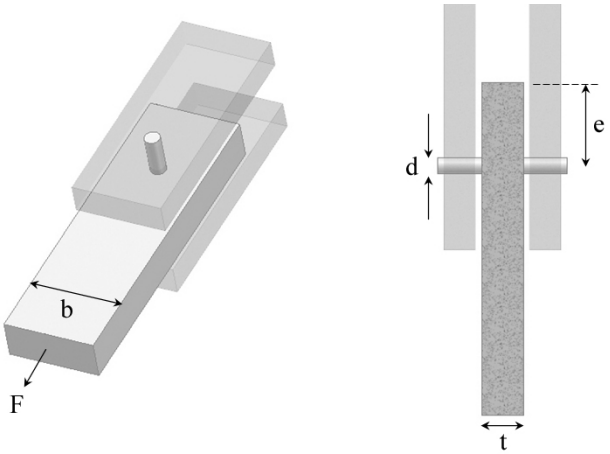

Figure 1. Double-lap mechanical joint

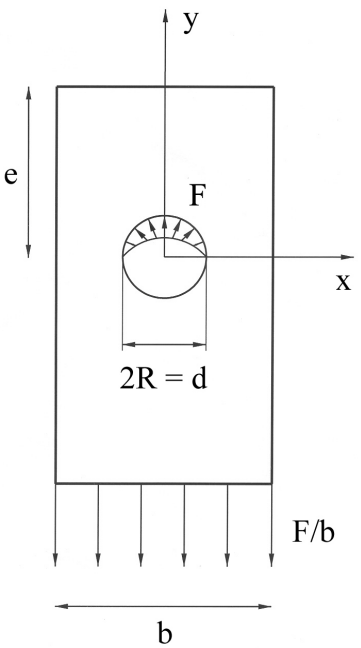

Figure 2. Geometry for the joint and boundary conditions

The method of complex functions (Lekhnitskii [20], Muskhelishvili [25]) for anisotropic materials is used to obtain the stress distributions. For plane stress situations in orthotropic plates the stresses can be expressed by means of derivatives of two stress complex functions $\varphi(z_1)$ and $\Psi(z_2)$:

$$\sigma_x = 2\mathbf{Re}\left\{\mu_1^2\varphi'(z_1)+\mu_2^2\Psi'(z_2)\right\} \quad (1)$$

$$\sigma_y = 2\mathbf{Re}\left\{\varphi'(z_1)+\Psi'(z_2)\right\} \quad (2)$$

$$\tau_{xy} = -2\mathbf{Re}\left\{\mu_1\varphi'(z_1)+\mu_2\Psi'(z_2)\right\} \quad (3)$$

where $\varphi(z_1)$ and $\Psi(z_2)$ are arbitrary functions of the complex variables z_1 and z_2 :

$$z_1 = x+\mu_1 y \quad (4)$$

$$z_2 = x+\mu_2 y \quad (5)$$

In general, the complex functions $\varphi(z_1)$ and $\Psi(z_2)$ can be estimated from the boundary conditions of the problem. The pertinent solutions for the pin-loaded hole in an elastically orthotropic or isotropic plate problem have been obtained by Echavarría [11] and Echavarría *et al*. [12] and are summarized here.

$$\varphi(z_1) = ALn\zeta_1+\Gamma_0(\zeta_1)+\frac{F}{4b}\frac{\mu_2}{\mu_1-\mu_2}\left\{\frac{R}{\zeta_1}-\frac{\mu_2}{\mu_1+\mu_2}z_1\right\} \quad (6)$$

$$\Psi(z_2) = BLn\zeta_2+\Xi_0(\zeta_2)+\frac{F}{4b}\frac{\mu_1}{\mu_2-\mu_1}\left\{\frac{R}{\zeta_2}-\frac{\mu_1}{\mu_1+\mu_2}z_2\right\} \quad (7)$$

$$\varphi'(z_1) = \frac{d\varphi}{dz_1} = \frac{d\varphi}{d\zeta_1}\frac{d\zeta_1}{dz_1}+\frac{F}{4b}\frac{\mu_2}{\mu_1-\mu_2}\left\{-\frac{R}{\zeta_1^2}\frac{d\zeta_1}{dz_1}-\frac{\mu_2}{\mu_1+\mu_2}\right\} \quad (8)$$

$$\Psi'(z_2) = \frac{d\Psi}{dz_2} = \frac{d\Psi}{d\zeta_2}\frac{d\zeta_2}{dz_2}+\frac{F}{4b}\frac{\mu_1}{\mu_2-\mu_1}\left\{-\frac{R}{\zeta_2^2}\frac{d\zeta_2}{dz_2}-\frac{\mu_1}{\mu_1+\mu_2}\right\} \quad (9)$$

where

$$\frac{d\varphi}{d\zeta_1} = \frac{A}{\zeta_1}+\frac{d\Gamma_0}{d\zeta_1} \quad (10)$$

$$\frac{d\Psi}{d\zeta_2} = \frac{B}{\zeta_2}+\frac{d\Xi_0}{d\zeta_2} \quad (11)$$

The values of complex constants *A* and *B* are found from:

$$A = A'' i \quad (12)$$

$$B = B'' i \quad (13)$$

$$B'' = \left(-\frac{F}{4\pi}\right)\div\left\{1-\frac{u_2}{u_1}\right\} \quad (14)$$

$$A'' = \left(-\frac{F}{4\pi}\right)-B'' \quad (15)$$

where u_1 and u_2 are constants determined by:

$$u_j = S_{11}\mu_j^2+S_{12}\ \ (j=1,2) \quad (16)$$

$\Gamma_0(\zeta_1)$ and $\Xi_0(\zeta_2)$ are the holomorphic parts of $\varphi(z_1)$ and $\Psi(z_2)$:

$$\Gamma_0(\zeta_1) = \frac{i}{4\pi(\mu_1-\mu_2)}\left\{\int_{\sigma=+1}^{\sigma=-1}\left[\frac{\mu_2 F}{4\pi i}\left(4Ln\sigma-\sigma^2+\overline{\sigma}^2\right)+\frac{F\omega}{4\pi}\left(\sigma^2+\overline{\sigma}^2-2\right)\right]\frac{\sigma+\zeta_1}{\sigma-\zeta_1}\frac{d\sigma}{\sigma}+\right.$$
$$\left.\int_{\sigma=-1}^{\sigma=+1}[\mu_2 F]\frac{\sigma+\zeta_1}{\sigma-\zeta_1}\frac{d\sigma}{\sigma}-\int_{\gamma}\left[\frac{\mu_2 F}{2\pi i}Ln\sigma\right]\frac{\sigma+\zeta_1}{\sigma-\zeta_1}\frac{d\sigma}{\sigma}\right\} \quad (17)$$

$$\Xi_0(\zeta_2) = \frac{i}{4\pi(\mu_2-\mu_1)}\left\{\int_{\sigma=+1}^{\sigma=-1}\left[\frac{\mu_1 F}{4\pi i}\left(4Ln\sigma-\sigma^2+\overline{\sigma}^2\right)+\frac{F\omega}{4\pi}\left(\sigma^2+\overline{\sigma}^2-2\right)\right]\frac{\sigma+\zeta_2}{\sigma-\zeta_2}\frac{d\sigma}{\sigma}+\right.$$
$$\left.\int_{\sigma=-1}^{\sigma=+1}[\mu_1 F]\frac{\sigma+\zeta_2}{\sigma-\zeta_2}\frac{d\sigma}{\sigma}-\int_{\gamma}\left[\frac{\mu_1 F}{2\pi i}Ln\sigma\right]\frac{\sigma+\zeta_2}{\sigma-\zeta_2}\frac{d\sigma}{\sigma}\right\} \quad (18)$$

where

$$\omega = \frac{1 - \sin \alpha}{\cos \alpha} \tag{19}$$

$$\alpha = \frac{\pi}{5}\left\{\frac{e-2d}{d}\right\} - \frac{\pi}{30}\left\{\frac{e-2d}{d}\right\}^2 \qquad 2d \le e \le 5d \tag{20}$$

$$\alpha = \frac{3\pi}{10} + \frac{\pi}{45}\left\{\frac{e-5d}{d}\right\} \qquad 5d \le e \le 14d \tag{21}$$

In this manner, stress functions $\varphi(z_1)$ and $\Psi(z_2)$ are completely determined. Evidently, with this analytical method, it is possible to estimate the stresses in any point of the orthotropic joint and to show the stress distribution around a pin-loaded hole in an elastically orthotropic plate. The effect of material properties and geometry of the joint can be determined analytically. Although it was developed for orthotropic composite materials, the presented approach is equally effective for analyzing mechanical joints involving solid wood and wood-based composites.

3. BRITTLE FAILURE OF A BOLTED TIMBER JOINT AND IMPROVING LOAD-CARRYING CAPACITY

The proposed model can be used to determine analytically the points of stress concentrations in the zone of contact between the fastener and the timber and predict the brittle modes of failure in dowel-type timber joints.

Let's consider, for instance, the stress distributions calculated for a wood element of a unit thickness *t* and width $b = 4d$ assuming the elastic properties of red spruce shown in Table 1. Table 2 summarizes the peak stresses τ_{xy} and σ_x at corresponding angles θ for red spruce calculated in this example. The calculated stresses are normalized by the average bearing stress $p = F/d$ and are shown along the hole edge as a function of angle θ (as defined in Fig. 3).

Table 1. Elastic constants (MPa) of red spruce (Wood Handbook [30])

E_x	E_y	G_{xy}	v_{yx}
470	11100	670	0,470

Table 2. Predicted peak stresses at a joint of red spruce

e/d	Shear stress at $\theta = 60°$ τ_{xy}/p	Perpendicular-to-grain stress at $\theta = 90°$ σ_x/p
2	0,80	0,52
3	0,50	0,20
4	0,34	0,04
5	0,31	0,01
7	0,28	-0,03
10	0,18	-0,13

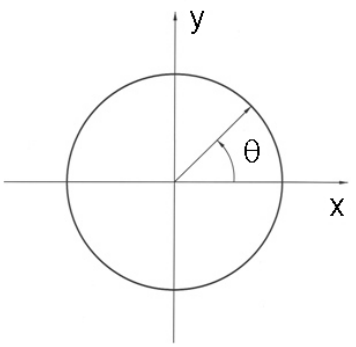

Figure 3. Angle θ

Avoiding completely tension perpendicular-to-grain and shear is not ever possible. If not placed properly, bolts may cause undesirable brittle failure in timber due to excessive tension perpendicular-to-grain. A possibility to avoid splitting and to guarantee a plastic joint behaviour is to reinforce the timber in the joint area. The tension stresses are then transferred by a reinforcement perpendicular-to-grain. Known methods to prevent splitting of timber members are reinforcements of the joint area with glued-on wood-based panels, pressed-on punched metal plates or glass fibre reinforcements. If wood

joint could be reinforced (Haller *et al*. [14], Haller and Wehsener [15], Blass and Bejtka [5], Chen [6], Hansen [16], Hockey *et al*. [17], Soltis *et al*. [28]), end distance requirements could be re-evaluated, which would allow more compact joints and an easier installation.

The approach presented in this study is to use self-tapping screws oriented perpendicular-to-grain as internal reinforcement. The reinforcement is shown in Fig. 4. Compared to the reinforcement methods mentioned, self-tapping screws are easier to apply and less expensive.

In this paper, splitting failure is assumed to occur as soon as the perpendicular-to-grain stress reached the strength perpendicular-to-grain of the wood. Basically, the perpendicular-to-grain strength can be improved by reinforcement. Reinforcement could be used locally in the vicinity of a bolt. Consequently, the cracks may be stopped at the position of the reinforcements and the bearing strength of the wood could be attained.

The analytical model presented allows predicting the load in the reinforcing screw. The force *Fs* acting in the screw is equal to the perpendicular stress σ_x multiplied by the area *As* on which the force acts.

The equation that describes the area *As*, considering the stresses between $y=R$ and $y=2R$, has the following form:

$$As = t\,R \tag{22}$$

The force acting in the screw is:

$$Fs = \left\{\left(\frac{(4+\pi)\,Fn\omega}{2R\pi^2}\right) - \left(\frac{Fk}{2b} + \frac{3Fk}{2R\pi}\right) - \left(\frac{\upsilon_{xy}F}{2R\pi}\right)\right\}\frac{As}{t} \tag{23}$$

In these circumstances local reinforcement can be very effective in ensuring a reasonable load-carrying capacity and stiffness and in providing the necessary ductility.

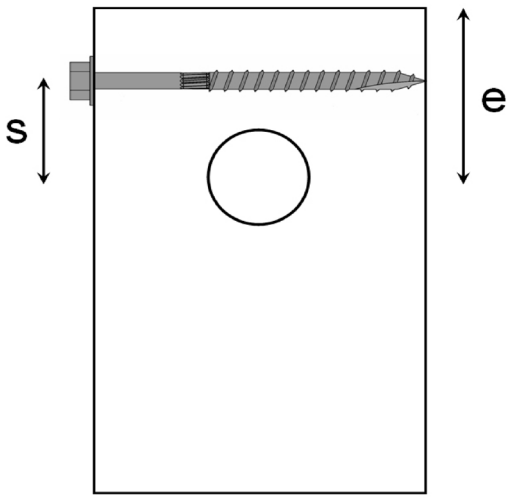

Figure 4. Reinforced bolted joint

4. EXPERIMENTAL VERIFICATION

Laboratory tests on reinforced and non-reinforced bolted timber joints loaded parallel to grain by a single bolt representing the geometry shown in Fig. 1 were performed to verify the predictions of the proposed analytical model. The bolts were 15,9-mm (5/8-in.) in diameter made of low carbon steel conforming to ASTM A307. Bolt lengths were selected to ensure that threads were excluded from bearing against the wood. The ratio of the wood member thickness to bolt diameter was small enough to induce failure in the wood, with minimum bending deformation of the bolt. Wood plates for the joints were cut from 38 by 89-mm (nominal 2 by 4-in.) red spruce kiln-dry lumber so that the joint area was free of defects. Tabla 3 and table 6 show the single-dowel joint geometry.

Prior to testing, the specimens were conditioned to attain 12 % equilibrium moisture content. Specific gravity based on oven-dry mass and volume at 12 % moisture content of the specimens varied

Table 3. Non-reinforced single-dowel joint geometry

Bolt diameter *d* (mm)	Edge distance *b/2* (mm)	Thickness *t* (mm)	End distance *e*	Number of replications
15,9	44,5	38,0	2*d*, 3*d*, 4*d*, 5*d*, 7*d* and 10*d*	53

Table 4. Mechanical properties of red spruce

Plate thickness *t* (mm)	Strength average (MPa)		
	σ_x Perpendicular-to-grain	σ_y Embedding	τ_{xy} Shear
38,0	3,80	29,7	8,80

from 0,37 to 0,41 as determined per ASTM D2395-02 [2]. Material shear strength parallel-to-grain and tensile strength perpendicular-to-grain were determined using ASTM D143-94 [1]. The shearing surface dimensions were identical for all shear strength parallel-to-grain tests. The dowel embedding strength for each bolt diameter was determined according to ASTM D5764-97a [3]. The material properties are summarized in Table 4.

The joints were tested with static load applied in tension parallel-to-grain using a universal testing machine in accordance with EN 26891:1991 [13].

Fig. 4 shows the reinforcing screw used in this study. A screw (GRK fastener 1/4" by 3½") with 90 mm of length, 6 mm of outer diameter and 70 mm of threaded length was used. The reinforcing screw is at a distance $s=d$ from the centre of the hole.

Tests were normally conducted on single-hole specimens which had the geometry described in Tables 5 and 7. During the course of this experimentation, 37 specimens were tested using reinforced joints with self-tapping screws. For comparison, 53 joints were tested without reinforcement perpendicular-to-grain.

Table 5. Experimental results and analytical predictions for non-reinforced single-bolted joints

Bolt diameter *d* (mm)	*e/d*	Experimental			Predicted			Comparison
		Number of replications	Average failure load *Fexp* (kN)	Standard deviation *(%)*	Failure load *F* (kN)	Average bearing stress *p* (MPa)	Prevalent failure mode	$\frac{(F-Fexp)}{Fexp}$ (%)
15,9	2	10	4,43	13	4,42	7,30	Splitting	-0,40
	3	8	12,1	7	10,6	17,6	Shear-out	-12,5
	4	10	17,3	4	15,6	25,9	Shear-out	-9,60
	5	10	18,2	9	17,2	28,4	Shear-out	-5,60
	7	7	20,5	7	17,9	29,7	Bearing	-12,5
	10	8	20,3	10	17,9	29,7	Bearing	-11,4

Table 6. Reinforced single-dowel joint geometry

Bolt diameter *d* (mm)	Edge distance *b/2* (mm)	Thickness *t* (mm)	End distance *e*	Number of replications
15,9	44,5	38,0	2*d*, 3*d*, 4*d* and 5*d*	37

Table 7. Experimental results and analytical predictions for reinforced single-bolted joints

Bolt diameter *d* (mm)	*e/d*	Experimental			Predicted			Comparison
		Number of replications	Average failure load *Fexp* (kN)	Standard deviation *(%)*	Failure load *F* (kN)	Screw load *Fs* (kN)	Prevalent failure mode	*(F-Fexp) / Fexp* (%)
15,9	2	10	9,76	10	6,65	1,10	Shear-out	-31,9
	3	9	12,7	25	10,6	1,10	Shear-out	-16,5
	4	9	17,4	5	15,6	0,30	Shear-out	-10,3
	5	9	18,4	10	17,2	0,10	Shear-out	-6,5

The number of replications, the summary of test results and comparison with the analytical predictions for each test configuration are given in Tables 5 and 7. The load-carrying capacities were predicted using the stresses obtained by the analytical model and the failure criteria presented above.

The effectiveness of reinforcement methods is studied along with the possibility of reducing the end-distance requirements. Test results in Table 7 showed that reinforcement had positive effects on the load-carrying capacity when the end distance *e* is shortest. The predominant failure mode in specimens loaded parallel to grain was in shear without plug-shear-out. Little evidence of wood crushing was observed. The screws prevent the cracks from further growing. Failure modes were affected by reinforcement; the propagation of crack was reduced. Generally, the crack propagation in non-reinforced joints was more pronounced than in the reinforced ones. The reinforced specimens with *e=2d, 3d, 4d* and *5d* failed mainly in shear as predicted by the model.

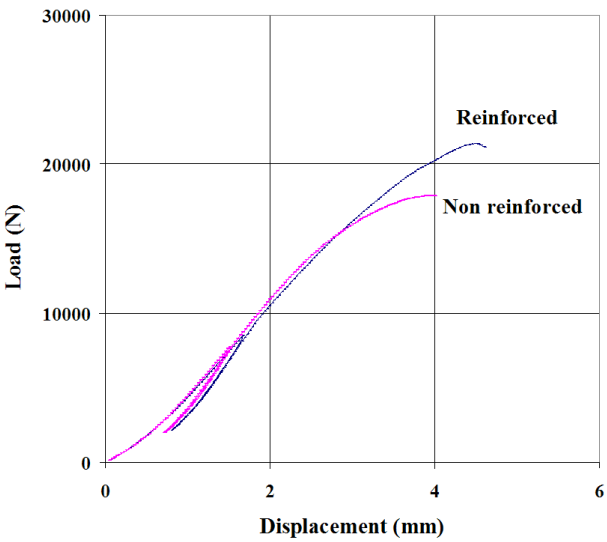

Figure 5. Load ~ displacement behaviour for reinforced and non-reinforced bolted joints.

(*d* = 15,9 mm, *b/2* = 44,5 mm, *t* = 38,0 mm, *e/d* = 5)

Fig. 5 shows the load-displacement curves for a non-reinforced and a reinforced joint. Table 8 shows the relation between load-carrying capacity of reinforced and non-reinforced joints. Particularly,

the load-carrying capacity increases 120 % for the *e=2d* reinforced specimens with 15,9-mm bolts. It is clear that the increase in load-carrying capacity is significant with the use of the reinforcing screws enabling smaller joints and significant savings in timber volume.

Table 8. Relation between load-carrying capacity of reinforced and non-reinforced joints

Bolt diameter *d* (mm)	*e/d*	Ratio of reinforced and non-reinforced load-carrying capacity (%)
15,9	2	120
15,9	3	4,68
15,9	4	0,78
15,9	5	1,03

5. CONCLUSIONS

The solution proposed here is entirely analytical and the most important results are compiled clearly in tables.

This study dealt with the analytical and experimental investigation of the effectiveness of self-tapping screws as means of reinforcing bolted timber connections loaded parallel-to-grain. Several equations are presented to calculate the load-carrying capacity of reinforced and non-reinforced timber joints.

The reinforced specimens showed a less catastrophic failure mode whereas the non-reinforced specimens failed in a brittle way. In reinforced joints it is observed some increase in embedding and ultimate strength, when compared with non-reinforced joints. It is also concluded that spacing and end distances can be reduced.

Ultimate loads from tests on wood plates loaded with a single bolt show a very good agreement with the calculated load-carrying capacities and predicted failure modes.

Nomenclature

A	complex constant
B	complex constant
b	width of plate
d	diameter of the hole
e	end distance
E_x	perpendicular-to-grain modulus of elasticity
E_y	longitudinal modulus of elasticity
F	resultant force
Fs	screw load
G_{xy}	shear modulus
p	average bearing stress
R	radius of the hole
s	screw distance
S_{ij}	elastic compliances of the plate material
λ	clearance
u_1 , u_2	constants
z_k	complex variable
μ_1 , μ_2	complex parameters of the first order
ν_{yx}	coefficient of Poisson
σ_x	perpendicular-to-grain stress
σ_y	longitudinal stress
τ_{xy}	shear stress
$\varphi(z_1)$, $\Psi(z_2)$	complex stress functions

ACKNOWLEDGMENTS

I thank CIBISA as well as the Université Laval for financial support of this project. The constructive comments of Daniela Blessent (Université Laval) and an anonymous reviewer are greatly appreciated and have helped to improve the manuscript.

REFERENCES

[1] American Society for Testing and Materials (ASTM) (2006). D143-94 Standard methods of testing on small clear specimens of timber. ASTM Annual Book of Standards. West Conshohocken, Pa

[2] American Society For Testing and Materials (ASTM) (2006). D2395-02 Standard test methods for specific gravity of wood and wood-based materials. ASTM Annual Book of Standards. West Conshohocken, Pa.

[3] American Society For Testing and Materials (ASTM) (2006) D5764-97a Standard test method for evaluating dowel-bearing strength of wood and wood-base products. ASTM Annual Book of Standards. West Conshohocken, Pa.

[4] Backlund J. and Aronsson C. Tensile fracture of laminates with holes. Journal of Composite Materials 1986;20:259-286.

[5] Blass H. J. and Bejtka I. Reinforcements perpendicular to the grain using self-tapping screws. WCTE 2004;1001-1006.

[6] Chen C. J. Mechanical behaviour of fiberglass reinforced timber joints. Ph.D. Thesis N° 1940, Swiss Federal Institute of Technology Lausanne EPFL, Switzerland, 1999.

[7] Collings T. A. and Beauchamp M. J. Bearing deflection behaviour of a loaded hole in CFRP. Composites 1984;15:33-38.

[8] Crews J. H. A survey of strength analysis methods for laminates with holes. Journal of the Aeronautical Society of India 1984;36:287-303.

[9] Dano M. L., Gendron G. and Picard A. Stress and failure analysis of mechanically fastened joints in composite laminates. Composite Structures 2000;50:287-296.

[10] De Jong T. Stresses around pin-loaded holes in elastically orthotropic or isotropic plates. Journal of Composite Materials 1977;11:313-331.

[11] Echavarría C. Analyse d'une plaque orthotrope avec trou: Application aux assemblages en bois. Ph.D. Thesis N° 2947, Swiss Federal Institute of Technology Lausanne EPFL, Switzerland, 2004.

[12] Echavarría C., Haller P. and Salenikovich A. Analytical study of a pin-loaded hole in elastic orthotropic plates. Composite Structures 2007; 79:107-112.

[13] EN 26891 Timber structures. Joints made with mechanical fasteners. General principles for the determination of strength and deformation characteristics 1991. (ISO 6891; 1983).

[14] Haller P., Wehsener J. and Birk T. Embedding characteristics of fibre reinforcement and densified timber joints. CIB/W18/34-7-7, Proceedings of meeting 34 Venice, Italy, 2001.

[15] Haller P. and Wehsener J. Use of technical textiles and densified wood for timber joints. 1st International RILEM Symposium on Timber Engineering, Stockholm, Sweden 1999;717-726.

[16] Hansen K. F. Mechanical properties of self-tapping screws and nails in wood. Canadian Journal of Civil Engineering 2002; 29: 725-733.

[17] Hockey B., Lam F. and Prion H. G. L. Truss plate reinforced bolted connections in parallel strand lumber. Canadian Journal of Civil Engineering 2000; 27:1150-1161.

[18] Jorissen A. Double shear timber connections with dowel type fasteners. Delft University Press, Delft; 1988.

[19] Kharouf N., McClure G. and Smith I. Postelastic behavior of single- and double-bolt timber connections. ASCE Journal of Structural Engineering 2005;131(1):188-196.

[20] Lekhnitskii S. G. Anisotropic plates. New York: Gordon and Breach Science Publishers; 1968.

[21] Li R., Kelly D. and Crosky A. Strength improvement by fibre steering around a pin loaded hole. Composite Structures 2002;57:377-383.

[22] McCarthy C. T., McCarthy M. A. and Lawlor V. P. Progressive damage analysis of multi-bolt composite joints with variable bolt-hole clearances. Composites Part B 2005;36:290-305.

[23] Moses D. M. Constitutive and analytical models for structural composite lumber with applications to bolted connections. Ph.D. Thesis, Department of Civil Engineering, The University of British Columbia, Canada; 2000.

[24] Moses D. M. and Prion H. G. L. Stress and failure analysis of wood composites: a new model. Composites Part B 2004;35:251-261.

[25] Muskhelishvili N. I. Some basic problems of the mathematical theory of elasticity. Noordhoff, Groningen; 1953.

[26] Okutan B. The effects of geometric parameters on the failure strength for pin-loaded multi-directional fiber-glass reinforced epoxy laminate. Composites Part B 2002; 33:567-578.

[27] Patton-Mallory M., Cramer S., Smith F. and Pellicane P. Nonlinear material models for analysis of bolted wood connections. ASCE Journal of Structural Gngineering 1997; 123(8):1063-1070.

[28] Soltis L. A., Ross R. J. and Windorski D. F. Fiberglass-reinforced bolted wood connections. Forest Products Journal 1998; 48(9):63-67.

[29] Wang H. S., Hung C. L. and Chang F. K. Bearing failure of bolted composite joints, Part I: experimental characterisation. Journal of Composite Materials 1996;30:1284-1313.

[30] Wood Handbook: Wood as an engineering material. Agricultural Handbook 72, Forest Products Laboratory, U.S. Department of Agriculture, Washington, 1987.

[31] Wong C. M. and Matthews F. L. A finite element analysis of single and two-hole bolted joints in fibre reinforced plastic. Journal of Composite Materials 1981; 15:481-491.

[32] Zhang K., and Ueng C. Stresses around a pin-loaded hole in orthotropic plates with arbitrary loading direction. Composite Structures 1985; 3:119-143.